© 2018 Chenxi Yan

EFFECT OF FATIGUE LOADING ON IMPACT RESPONSE OF RAT ULNA

BY

CHENXI YAN

THESIS

Submitted in partial fulfillment of the requirements
for the degree of Master of Science in Mechanical Engineering
in the Graduate College of the
University of Illinois at Urbana-Champaign, 2018

Urbana, Illinois

Adviser:

Assistant Professor Mariana E. Kersh

Abstract

Stress fracture is a common injury among athletes, such as basketball players. The occurrence of stress fracture is a consequence of both fatigue and impact loading of the bone that will potentially threat athletes' careers. Scientists and engineers have studied the fatigue properties of many engineering materials, and more recently biological materials. Investigating the role of fatigue on impact properties has received much less attention in bone. In this study, cyclic axial compressive loading was applied in vivo on the right ulnae of sixteen rats (Sprague-Dawley, Charles River), and the left served as contralateral control. The animals were divided into two groups: one day of rest before they were sacrificed and the other seven days. Afterwards, the ulnae were harvested and potted in epoxy and then scanned using micro-Computed Tomography (CT). Impact tests were performed using a customized figure where the impact energy was normalized for all specimens and following impact the specimens were re-scanned using micro-CT scans. There was no significant change in bone volume between the control (mean = 7.01 $\pm$ 0.61mm^3) and loaded (mean = 6.63 $\pm$ 0.19mm^3) ulnae in the group with one day rest (p = 0.28). However, after seven days of rest, the average bone volume increased by 4.35% among the control ulnae (mean = 7.32 $\pm$ 0.49mm^3), and 15.10% among the loaded (mean = 7.63 $\pm$ 0.47mm^3). The increase in volume was attributed to woven bone formation and was visually confirmed from the micro CT images. The peak impact force was 37.5% higher in the control (mean = 174.96 $\pm$ 33.25N) specimens than the loaded (mean = 130.34 $\pm$ 22.37N). Our data is limited to some degree by the sample size and two specimens fractured after the cyclic loading which further decease the sample size. Future work should investigate the effect of different rest times. This study indicated that cyclic fatigue loading had a negative impact on bone's impact response. Bones that experienced fatigue loading became less stiff and resulted in lower peak forces, and an increased fracture rate when subjected to impact. Rest time was crucial to the recovery of fatigue damage. Seven days rest decreased the fracture rate by 66.67%. If more rest time was given, the peak force could return to the same level as the control or even higher as new bone would possibly mineralize. This study can provide a baseline guidance of the training, competition and rest arrangement to minimize the risk of stress fracture and prolong athletes' careers.

Acknowledgements

I would like to express my gratitude and thanks to Professor Mariana Kersh for providing the opportunity for me to work on this project, and for her time and tireless support in helping me complete this thesis. I also want to express my appreciation to all the members from Tissue Biomechanics Lab for their assistance and contributions for my research, especially to Huyunggwi Song who devoted a great amount of time and energy helping me complete the experiment. And finally, thank you to my parents who support me to study abroad in all these years, and Zhongyu for supporting me through it all. Additionally, I would like to express my special thanks to Dr. Stuart Warden for lending me the experimental apparatus to complete this project.

Contents

1 Literature Review

1.1 Bone structure and composition

The adult human skeleton consists of 206 individual bones. Traditionally, skeletal bones are classified as four main types: long bones such as the femur and humerus, short bones (carals), flat bones (scapula), and irregular bones (coxae). In healthy living bone, on the outer surface is a membrane called the periosteum where blood vessels and nerves pass into the bone. The hard, outer shell of bone is known as cortical bone and makes up approximately 85% of the total skeleton [1]. The inner region is filled with trabecular bone at the epiphyses of long bones and throughout smaller bones (Figure 1). Trabecular bone is a complex and heterogeneous material, and the elastic and strength properties vary widely across anatomic sites [35]. Trabecular bone has a porosity up to 90% but it is much more flexible and suitable for metabolic activities [39].

The strength of bone at a given time in life is determined by the factors that influence the gain of bone during growth and those influence bone loss[56]. Bone needs to be stiff in order to provide support but also tough and flexible in order to absorb energy. These functions are dictated by a composite structure comprised of inorganic mineral crystals (33-43% bone volume), organic collagen fibers (32-44% bone volume), and water (15-25% bone volume) [41]. The crucial material in the mineral composition of bone is hydroxyapatite (HA) consisting of calcium and phosphate. In fact, 99% of the body's calcium is stored in skeleton. The reason that bone has heterogeneous material is partially due to the orientation of different layers of collagen fibers. Bone has the ability to adapt to different mechanical usage by changing its mass and structure[26]. Bone bone mineral density (BMD) is the amount of bone mineral in bone tissue, and is used in clinical medicine as an indirect indicator of osteoporosis and fracture risk.

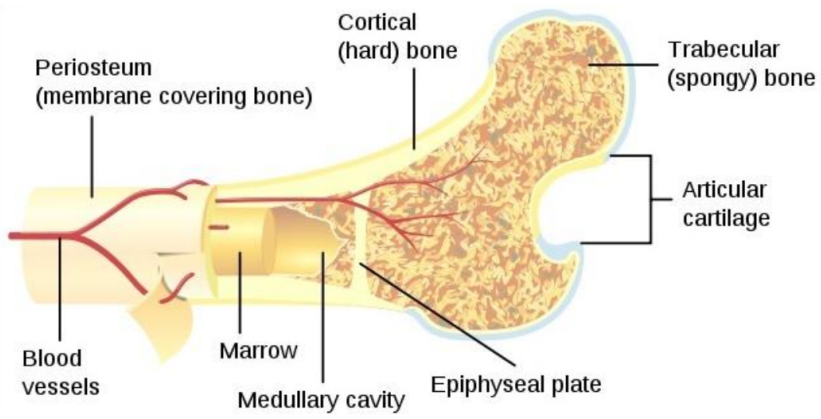

Figure 1: Bone structure. Cortical bone and trabecular bone can be recognized based on the location and their structures. The hard outer shell is made of cortical bone, and trabecular bone consists of trabeculae

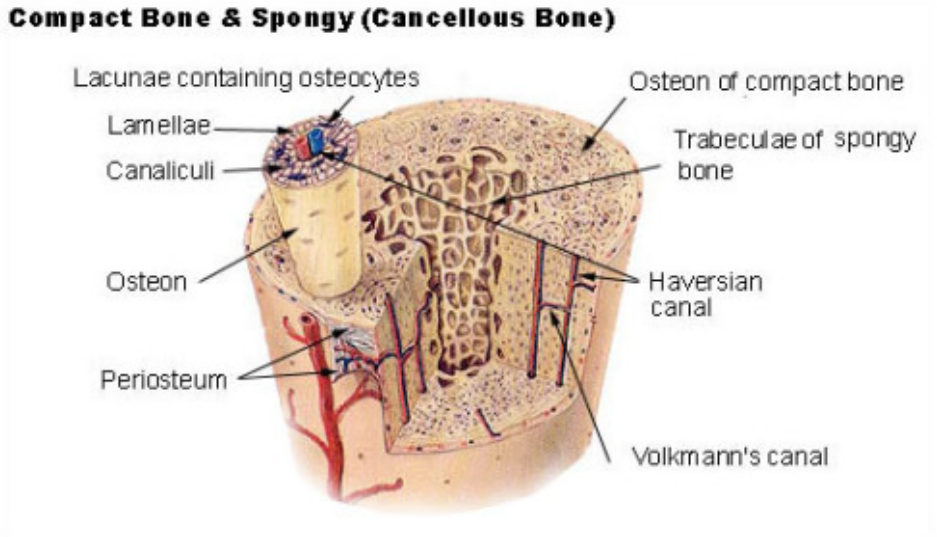

Figure 2: microstructure of bone. Bone as a biological material has a very unique hierarchical structure consisting of bundles of collagens, and canals, including Haversian canal system and Volkmann's canal system in two orthogonal directions.

1.2 Cortical bone structure

Cortical bone is covered by a periosteum on its outer surface and an endosteum, which is a thin vascular membrane of connective tissue, on its inner surface[40]. Similar to many other biological materials, cortical bone has a hierarchical structure. It consists of multiple microscopic columns that are made of osteons which are 250 microns in diameter and run parallel to the long axis of cortical bone in long bones. Each column consists of layers of lamalle which house the osteoblasts and osteocytes around a central Haversian canal. In contrast, Volkmann's canals are perpendicular to the Haversian canals and connect the osteons together. The nature and location of the bone cells will vary as bone remodeling proceeds [23].

1.3 Trabecular bone

Trabecular bone is less dense than cortical bone and thus has a higher surface area-to-volume ratio than cortical bone. It is weaker but more flexible. Trabecular bone is also highly vascular and contains red bone marrow where the production of blood cells occurs. Trabecular bone is often aligned in the same direction as the mechanical load experienced by bone. The trabaculae is composed of a network of rods and plates elements that together result in a spacious structure that allows for blood vessels (Figure 3).

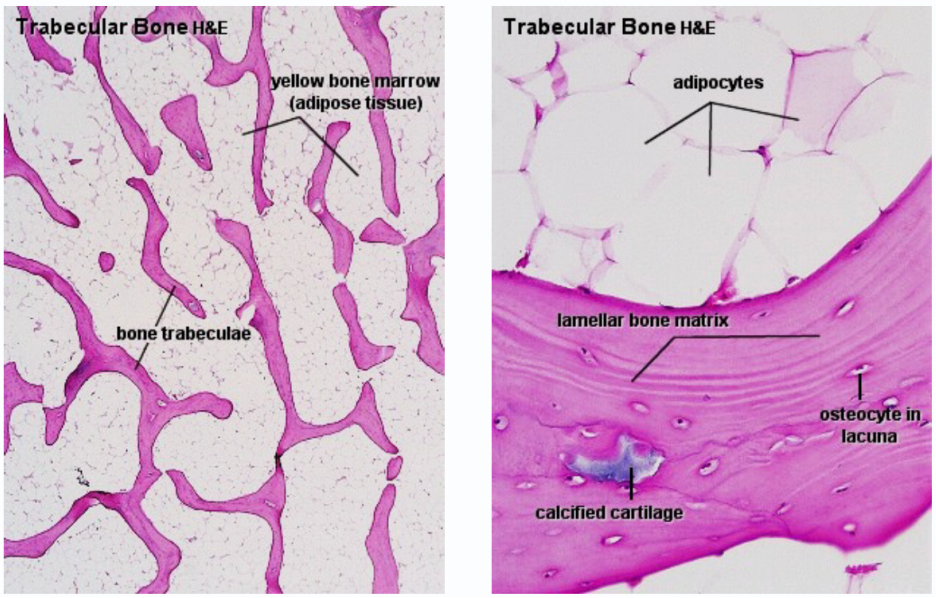

Figure 3: Histology of trabecular bone. Trabecular bone is the internal tissue of the skeletal bone and is an open cell network structure. It consists interconnected trabeculae and has higher sueface-area-to-volume ratio and a more flexible structure than cortical bone. http://www.lab.anhb.uwa.edu.au/mb160/CorePages/Bone/Bone.htm .

1.4 Bone fatigue and stress fractures

1.4.1 Fatigue

Fatigue is defined as the degradation of mechanical properties leading to material or component failure under cyclic loading[12]. Under cyclic loading, the material may fail at stress levels that are less than those required to cause static failure. The study of cyclic behavior of materials can be divided into three categories: stress-life approach, strain-life approach and fracture mechanics approach. All three approaches have their benefits and limitations. Traditionally, the behavior of a material under fatigue is described by the classical "S-N" curves, where S is the stress and N is the number of cycles to failure (Figure 4).

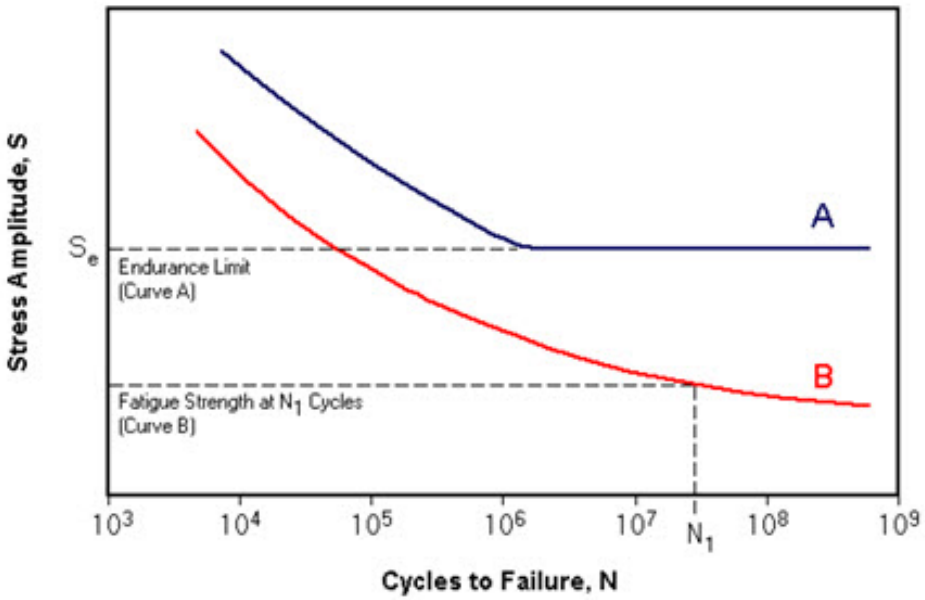

Figure 4: S-N Curve of 2 types of engineering materials[12].

It is known that the fatigue behavior of composite materials is complex and is characterized by the gradual loss of stiffness and strength under cyclic loading. Metals and some composite materials exhibit similar loading curves. However, the micromechanical events at yield and post-yield for metals are very different from those of composites. Yielding in metals is caused by plastic flow and is accompanied by the formation of a plastic slip line. When a metal specimen is loaded into the post-yield regime, unloaded, and subsequently reloaded, it may exhibit little or no loss of stiffness and ultimate strength. For composite materials, the post-yield regime is caused by multiple damage modes such as microcracking, debonding, void growth and fiber damage. A composite material under cyclic load will typically exhibit a loss of stiffness and degeneration of ultimate strength [10].

1.4.2 Fractures in bone

Stress fractures are small cracks in bone and are often caused by overuse or repeated loads. Stress fracture may also occur when bone is weakened by disease such as osteoporosis. The formation of microcracks in the skeletons of large animals, including humans, is due to fatgiue failure at the microscopic level and is usually caused by physiological cyclic loading [46, 20]. The accumulation and coalescence of microcracks play an important role in the pathological weakening of the skeleton[6]. A stress fracture represents the inability of a bone to withstand repetitive bouts of mechanical loading, which results in structural fatigue (fatigue failure) and the resultant signs and symptoms of localized pain and tenderness. Stress fractures often occur during prolonged exercise. Hence, it is common among athletes and military personnel (Figure 5).

Evans and Lebow [16] conducted the first experiment to determine the fatigue life of compact bone specimens from human femur, tibia, and fibula using flexural fatigue tests. The fatigue life in their study was shown to vary from 4.70 - 6.54 $\times 10^6$ cycles. Unlike most engineering materials, a remodeling response to fatigue is inducible in bone with negligible basal remodeling[52]. This remodeling response makes in vivo mechanical test much more complicated and needs further investigation.

Figure 5: Stress fracture in tibia.

1.5 Bone modeling and remodeling

Osteogenesis can occur through the formation of woven or lamellar bone. In the post-natal skeleton, woven bone forms when there is a need for rapid mineral deposition such as in distraction osteogenesis, fracture healing and stress fracture repair [28, 37, 27, 48]. Woven bone is characterized by relatively poor organization, low mineral density and high cellularity [37]. In contrast, lamellar bone forms at a slower rate during normal skeletal growth and in response to mild anabolic stimuli. Lamellar bone is highly organized, denser and has fewer cells compared to woven bone.

There are several 'rules' relating mechanical loading and cortical bone formation that are widely accepted. First, dynamic loading induces a remodeling response but static loading does not[24, 29]. Second, there exists a minimum strain threshold below which there is no change in bone formation whereas loads above this threshold increase bone formation in a dose-dependent manner[32, 45]. Third, the anabolic effects of adaptive loading plateau after a relatively low number of cycles. Woven bone

formation occurs when the mechanical loading generates hyperphysiological strain or induces bone damage[22]. Under conditions where loading produces discrete bone damage, robust woven bone formation ensues. Although it appears disorganized, woven bone formation is a well-regulated response to extreme conditions including the 'need' to accrue bone at a faster rate than can be accomplished by lamellar bone formation. Despite the obvious difference in histological organization, lamellar and woven bone can be formed at the same time on contiguous segments of the bone surface.

1.6 Cyclic loading of rat bone

The nature of bone makes it a unique composite material and thus bone has drawn the attention from many scientists. Due to the difficulty of in vivo human experiment, rats are often used as a model organism for many studies related to bone biomechanics. Specifically, their genetic, biological and behavior characteristics closely resemble those of humans, and many symptoms of human conditions can be replicated in rats. Fatgiue tests are usually conducted by applying cyclic loads with various magnitude to a number of identical specimens while recording the number of cycles to failure[10]. Axial compressive loading has become the gold standard for studying mechanically induced bone formation in rats due to mechanical loading.

Bone fatigue fracture in vivo is a complex phenomenon in which both mechanical damage and biological repair proceses play an important role[10, 11, 21, 38, 42, 43]. The bone remodeling process may act in sufficient time to repair the damage and maintain the bone structure if the fatigue micro-damage accumulates at a relatively slow rate[8]. In the case of damaging fatigue loading, an apoptotic osteocyte response occurs in the regions near newly developed microcracks [13, 54], followed by osteoclastic bone resorption in damaged regions 7-10 days after loading among the rats [5, 36]. In addition, robust periosteal woven bone formation response has been observed following damaging fatigue loading[25].

Cyclic loading of the rat forelimb has been used to generate bone damage resulting in ulnar stress fractures. After the damaging fatigue loading, there is a robust repair response characterized by periosteal woven bone formation near the damaged region[48, 14, 52]. According to Mark Forwood's research[19], a single bout of loading was sufficient to significantly increase bone formation parameters at the endosteal surface of rat tibiae. From a methodological perspective, ulna can be fatigued more easily in vivo [26, 5, 52, 25]. Supraphysiological cyclic axial compressive loading of the ulna in vivo has been used to induce bending with consequent fatigue and micro-damage (Figure 6)[5, 52, 26]. Others have investigated cyclic four-point bending on bone to investigate the change in mechanical properties (Figure 7)[48, 49]. Previous studies found that cyclic compression or bending test can generate microcracks that lead to different levels of stress fracture or complete failure of the bone,

and induce responses on cellular level to remodel and repair the damaged bone. However, the impact response of the bone following moderate fatigue damage do not receive much attention, and this study investigates this overlooked situation.

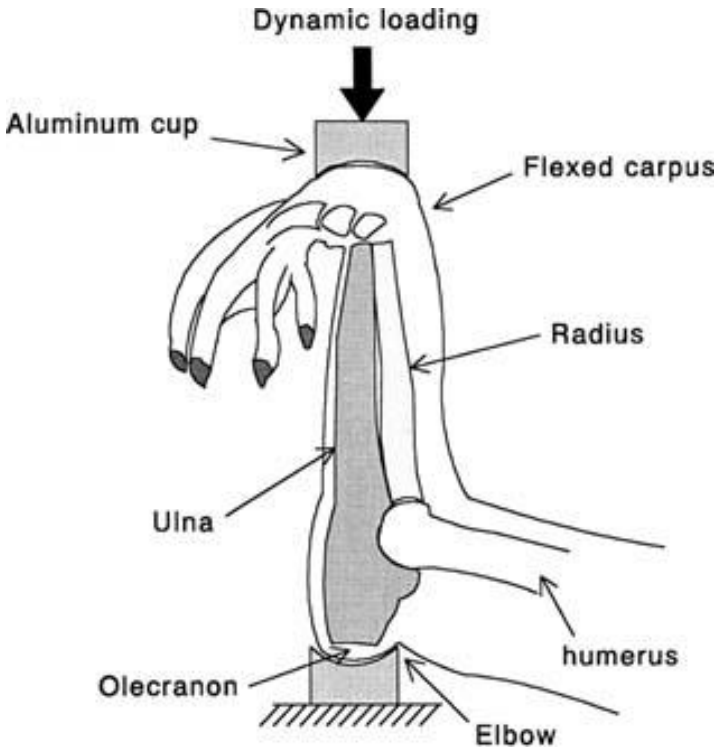

Figure 6: Schematic diagram of the ulna loading system. The forearm is held in cups between the flexed carpus and the olecarnon. The ulna is loaded through the carpal joint and overlying soft tissue. The load is applied through an actuator and the load cell at the elbow end can record the force data. Due to the geometry of the ulna, the axial loading induces bending along the diaphysis.

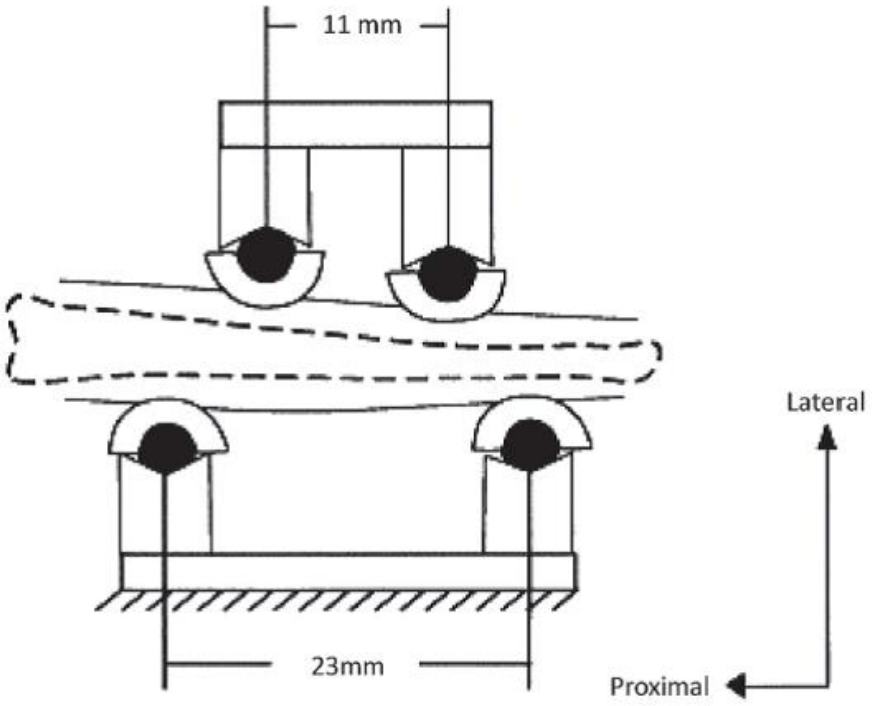

Figure 7: Schematic of four-point tibial bending. Bottom fixed points support the leg; top contact points displace downward. Four-point bending is also considered one of the standard method to test the mechanical properties of bone specimens.

1.7 Impact loading

Scientists and engineers have long been studying the mechanical properties of existing materials, and one of which is impact response. While there is a large amount of information available regarding the response of inanimate material, there is much less knowledge regarding the impact properties of biological material. Bone is a natural material designed for experiencing cyclic loading and impact forces associated with normal human locomotion, and has been robust in even more extreme conditions among athletes and military recruits. In the human body, cartilage and synovial fluids serve to spread and absorb impact forces as well as lubricate joints and minimize friction. In general, a stiff object is able to transfer most of the external impact, while a less stiff object would absorb and store part of the energy, for example, springs. When this energy exceeds a certain value, the object will likely fail.

Assessing the impact response of biological materials can provide engineers and scientists insights of the failure modes in both macro and micro levels. There is still considerable work that should be done to understand the exact nature of the cause and relationship between impact force and damage formation[17], as scientists have paid more attention to low velocity impact on engineering and biological material (Figure 8). Shyr and Pan studied the low velocity impact behavior and the damage characteristics in different fabric structures with various thickness of laminates[47]. They pointed out

that layer number is one of the important parameters for the energy dissipation mechanism in composite materials[17]. Since one of bone's main function is to support our body during activities and it has a hierarchical structure, it is a naturally excellent material for absorbing impact load.

Enns-Bray conducted an experiment using bovine trabecular bone to quantify the effect of strain rate on modulus of elasticity, ultimate stress, failure energy, and minimum stress of trabecular bone in order to improve the biofidelity of material properties used in dynamic simulations of sideways fall loading on the hip [15]. Using a drop tower experiment, they quantified the mechanical behavior of bovine trabecular bone at intermediate strain rates, from which new constitutive equations were derived that describe the mechanical properties of trabecular bone as a function of density, anisotropy, and strain rate. They found that the modulus, failure energy and minimum stress of trabecualr bone were significantly associated with strain rate, while the ultimate stress was significantly associated with degree of anisotropy (DA). They also indicated that strain rates ranging from 30 to 168/s had a small effect on the ultimate stress of bovine trabecular bone. It was the first study that using experimental data of loading rates between 10/s and 200/s to correlate methematical models of trabecualr density, anisotropy, and strain rate [15].

However, when bone is fatigued, the microstructure is damaged and the laminates or layers of collagen may be compromised. At the same time, the repair process is also activated to recover the tissue from damage. Impact loading on fatigued bone can provide insight related to how fatigue damage and the remodeling process of the bone can affect its impact response. It may also provide a method for modeling the high impact associated with athletes and military recruits who may endure intense bouts of activity (overuse) but may not receive enough rest.

Figure 8: Impact test machine. Weight will be dropped from the top onto the testing specimen. Most studies focused on low velocity impact which is more common than high velocity impact

1.8 Current Results

It has been shown that small changes in the structural properties of the rat ulna increases its fatigue resistance more than 100-fold [55] . This indicates that a moderate exercise program may be an effective preventative strategy for stress fracture recovery and strengthens bone. Seminal work by Carter and Hayes[9] showed that both the material and structural properties of bone directly influence its fatigue properties. Studies have also shown that stress fracture susceptibility is directly related to the structural properties of the skeleton. Subjects with lower bone mass and smaller bones were at greater risk of stress fracture than those with higher bone mass and larger bones[2, 3, 4, 31]. Modification of bone's mechanical and structural properties through the exploitation of the adaptive ability of bone may be used as a means of influencing an individual's risk, because stress fracture risk was largely influenced by the skeletal properties. Applying a mechanical loading program is one way to achieve this purpose. While repetitive mechanical loading can lead to skeletal fatigue, it can also act as a potent anabolic stimulus[51]. A recent study conducted by Enns-Bray successfully tested the compressive properties of trabecular bone at strain rates above 10/s. Based on four different impact speeds, with constant energy, they were able to find significant different strain rates between groups. The majority of specimens failed due to buckling of an entire transverse plane of bone tissue orthogonal to the loading axis at different heights along the gauge length, while high-density specimens had smaller localized failure zones [15]. Although the fatigue damage of rat ulna has been well studied in both structural and cellular level, the role of fatigue driven remodeling and rest on the impact strength of bone has not been explored.

2 Introduction

2.1 Motivation for Studying Fatigue Loading and Impact Loading

The skeleton serves to support and protect vital organs, and transfer the repeated forces associated withe the musculoskeletal system. Strains in the human tibia during walking and running are well below the fatigue threshold [30], yet stress fracture occur with repeated loads. These fractures are a result of microscopic cracks that form at stress concentration regions such as the surface and interfaces of constituents. Eventually, the crack will reach a critical size, propagate, and potentially cause fracture suggesting that momentary high stress or strain may occur during some vigorous activities[7]. For many athletes and military recruits, they have to perform a large amount of vigorous exercises which generate increased impact forces, which can cause fatigue damage in bone and is complicated by insufficient rest. If bone tissue damaged by microcracking is not repaired by remodeling, then usually a fatigue fracture will develop[13, 6].

The biological response of bone to fatigue micro-damage may be influenced by the type of induced damage. Carter & Hayes demonstrated that fatigue micro-damage is markedly different in repeated compressive stress than tensile stress[8]. Professional athletes usually train with high volume and intensity, but they do not always have enough time to recover. As a result, there could be micro-damage accumulated in their bones, such as the tibia, but they still have to perform certain exercise regardless of their conditions. Hence, the fatigue behavior could play an important role in their follow-up loading conditions. Moreover fatigue fractures are an important health problem in humans, particularly in the elderly, individuals with metabolic bone disease, such as osteoporosis, and in athletes. It is generally accepted that accumulation and coalescence of microcracks is an important determinant of whole bone structural properties, but this relationship remains unclear, and few data are available from experimental or naturally occurring fatigue fracture models [14].

The current standard method to load rat ulna to fatigue includes cyclic axial compression or four-point-bending. Histomorphometry and microCT are most widely used to examine the internal structure of the bone with different length scales. However, few studies have investigated the combination of fatigue and impact loading. Although many athletes continue to perform sports with potentially fatigued bones, there is the need to investigate how, and to what degree fatigue loading will affect the impact response of bone. A clear understanding of the material response of bone tissue to fatigue and impact loading can provide insights into the in vivo bone fatigue process[8].

2.2 Study Goals and Hypotheses

Understanding the relationship between the cortical response of bone to fatigue, and resulting mechanics, is necessary to identify the degree to which fatigue loading associated with vigorous activity disposes bone to impact-initiated failure. Therefore, using a rat model of fatigue, the purpose of this study was to investigate the effect of fatigue loading on the impact response of rat ulna.

Hypotheses:

The first hypothesis of this study is that a single bout of cyclic loading on rat ulna is enough to induce fatigue damage, and there will be woven bone formation as a remodeling response to the load if 7 days rest was given to the subject.

The second hypothesis is that the fatigue will induce micro-damage to the bone, reducing the stiffness. Impact loading can also damages the bone, regardless of fatigue. However, the formation of woven bone will increase the resistance to impact loading of the loaded bones.

3 Materials and methods

3.1 Study design

Sixteen Sprague-Dawley rats were acquired at 4 months of age weighing 432 ± 30 grams (Charles River, Wilmington, MA, USA). The rats were divided into two groups: (1) fatigue loading with one day of rest and (2) fatigue loading with seven days of rest. Rats were provided with food and water ad libitum. All procedures were approved by the University of Illinois Institutional Animal Care and Use Committee (IACUC). The general procedure of the experiment was presented in the diagram below.

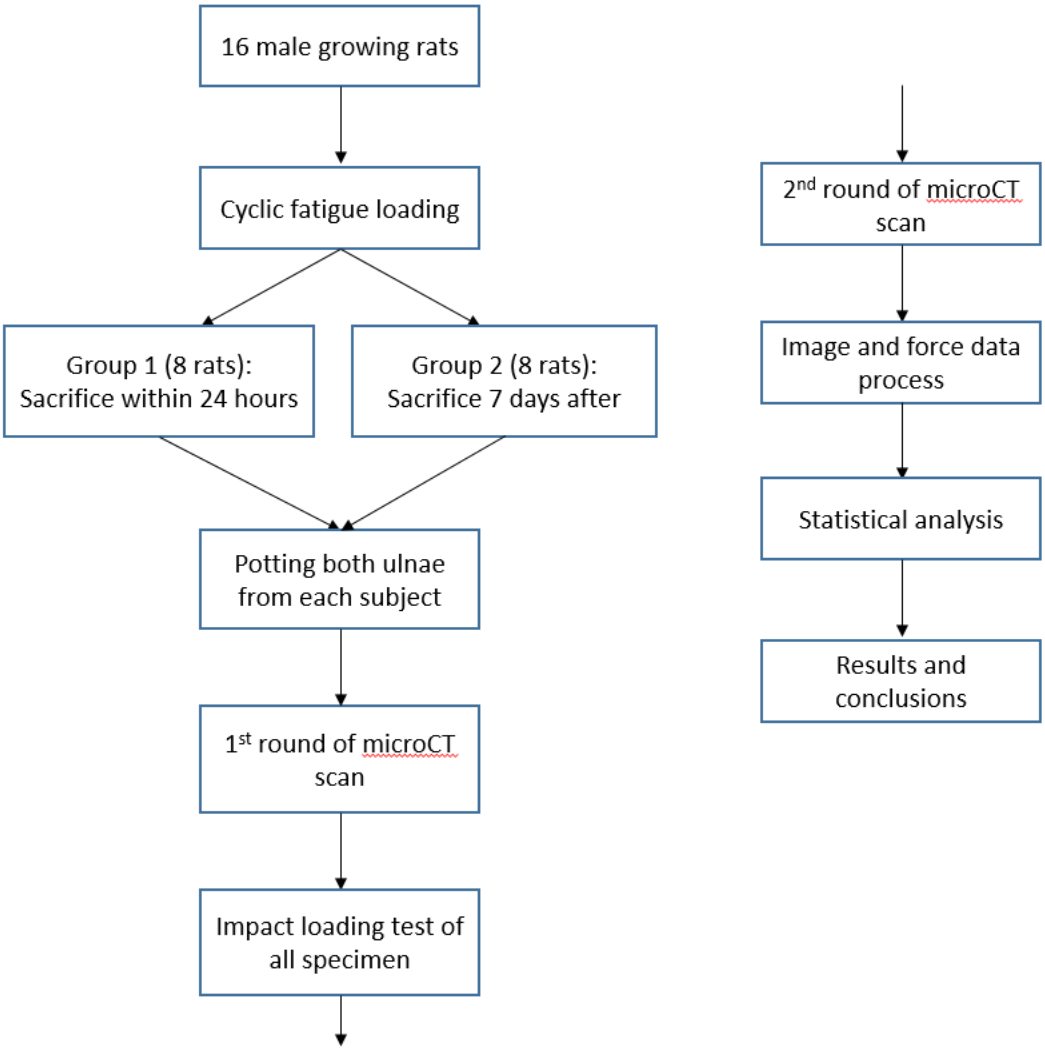

Figure 9: General methodology of the experiment.

3.2 Fatigue loading

Under continuous anesthesia, the rats were placed on a bed between the actuator and load cell (Figure 10). During loading, the right forelimb was carefully positioned with the elbow and volar flexed carpus placed in potted aluminum cups. The ulna were loaded axially in compression across the carpus and the olecranon process based on methods described previously[53, 5, 25].

Load was applied using a dynamic oscillation apparatus (Bose Wintest, Bose corporation, Framingham, MA, USA). The apparatus for cyclic loading includes a computer station, Bose Win-test load cell and actuator. The actuator was force-controlled and was programmed to produce cyclic fatigue loading with frequency of 2 Hz as a haversine waveform. All rats were anesthetized with 1-3% isoflorane during the in vivo loading process, and pain relief (Meloxicam, 2mg/kg) was given through subcutaneous injection immediately after loading. The forelimb was be preloaded to 2N to secure solid contact within the cups. At the beginning of each loading session, the forelimb underwent a pre-load session of 20 cycles at 5N, 10N, 15N and 20N.

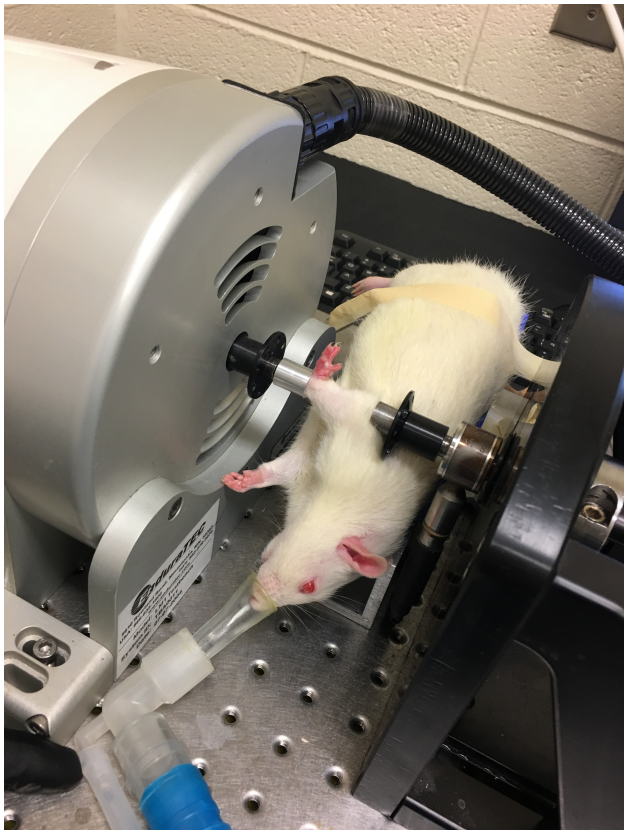

Figure 10: Cyclic load equipments consist of a computer, an actuator, and a load cell. It was important to secure the ulna into the caps. The concentration of the isoflorane should not exceed 3% for safety purpose.

Fatigue loading was then performed at a peak force of 0.055N per gram of body weight. The mean value of increased peak displacement that would cause failure was determined as 2mm relative to the tenth cycle [53]. Loading was stopped when the peak displacement reached 0.75mm ± 0.20mm and was limited to a maximum of one hour. The non-loaded left forelimbs served as internal contralateral controls.

3.3 Mechanical impact testing

Twenty-four hours after the completion of fatigue loading, eight rats were euthanized and the ulna were dissected within 24 hours. The other group were euthanized and dissected seven days later. All ulnae were potted with epoxy in customized fixtures at both ends(Figure 11A & B). The fixtures were designed to allow for repeated scanning within a micro-CT scanner before and after impact testing, and included flat surfaces to receive the impact load. However, due to the lack of skill in potting the bone with instant epoxy, two subjects in each group did not produce stable specimens after potting and were discarded.

A drop-tower apparatus was designed to hold the potted ulna for impact testing (Figure 11C). Aluminum plates served as the base upon which a load cell (ATI Industrial Automation, FT17980) was secured to record impact load (sampling frequency = 40 kHz). A 3D printed plastic fixture was fixed on top of the load cell to attach the potted specimen to the load cell. A pair of aluminum square U-channel tubes were used as side rails to guide the weight after release. A plastic cap at the top of the channel was used to secure the side rails and avoid lateral distortion during testing.

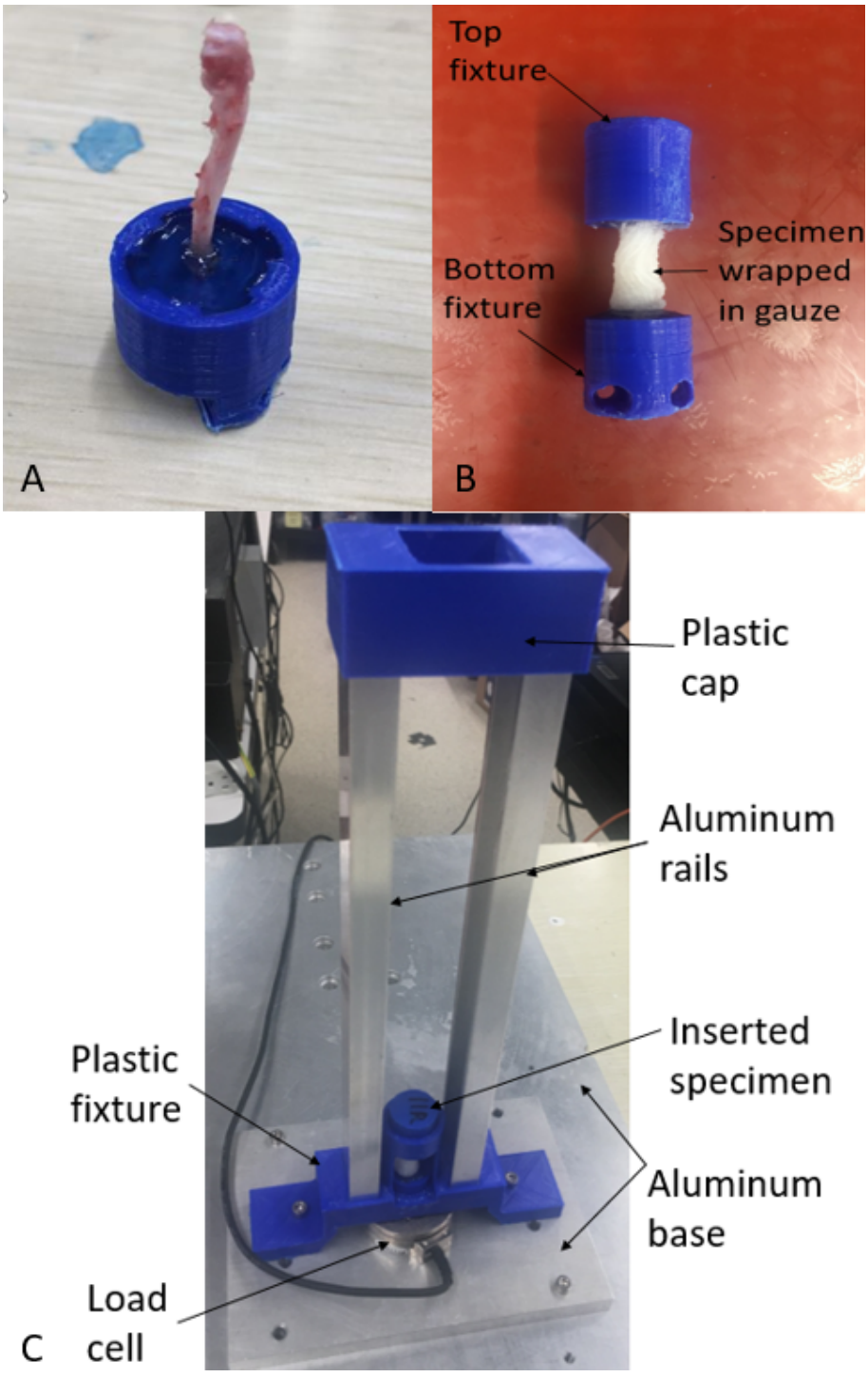

Figure 11: A:Base fixture and potted bone. The epoxy took about 5 minutes to cure. Before that, it cannot be wrapped with gauze soaked with PBS solution until both end of the specimen were completely solidified. B:Completed potting of ulna. After both ends were secured, the gauze can be wrapped onto the bone to rehydrate. C:Impact tower is customized for this experiment. The specimen can be inserted into the fixture and sit on top of the load cell.

The total potential energy due to landing from 0.2m was used to normalize the total potential energy due to impact across each specimen accounting for specimen weight as shown in the equation. Where PE was total potential energy, m was mass of each subject in kg, g was gravity constant, $9.8 m/s^2$, and h was 0.2m.

$$PE = 0.175 * m * g * h \tag{1}$$

High-speed cameras (Panasonic DMC-FZ200, 120 frames/s) were used to record the impaction of each sample.

3.4 Micro-Computed Tomography scans and image processing

Prior to impact testing, microCT scans (average isotropic resolution approximately 5 μm, 55kV, 8W, 145mA, Xradia MicroXCT, Xradia Incorporation, Concord, CA, USA) of each specimen was acquired. A second set of images were obtained following impact loading. Each scan acquired 996 slices (file format = Digital Imaging and Communications in Medicine, DICOM) of the diaphysis with each image containing 996x1016 voxels. The time interval between the two scans was less than 48 hrs, and scan settings were kept the same for all specimens.

All images were binarized using ImageJ(1.52e, Wayne Rasband, National Institute of Mental Health, Bethesda, MD, USA). First, the background was subtracted and an automatic threshold was applied to generate binarized images. The binarized images were then imported to Matlab (R2016b, Mathworks, Natick, MA, USA) to invert the images and generate images of only the internal cortical vascular canals for skeletonization.

The skeletonization process generated a 3D volume view of the internal structure of a bone given the stack of binarized images of the canals (Figure 12). Upon generating the volume view, the number of segments within the skeleton was calculated.

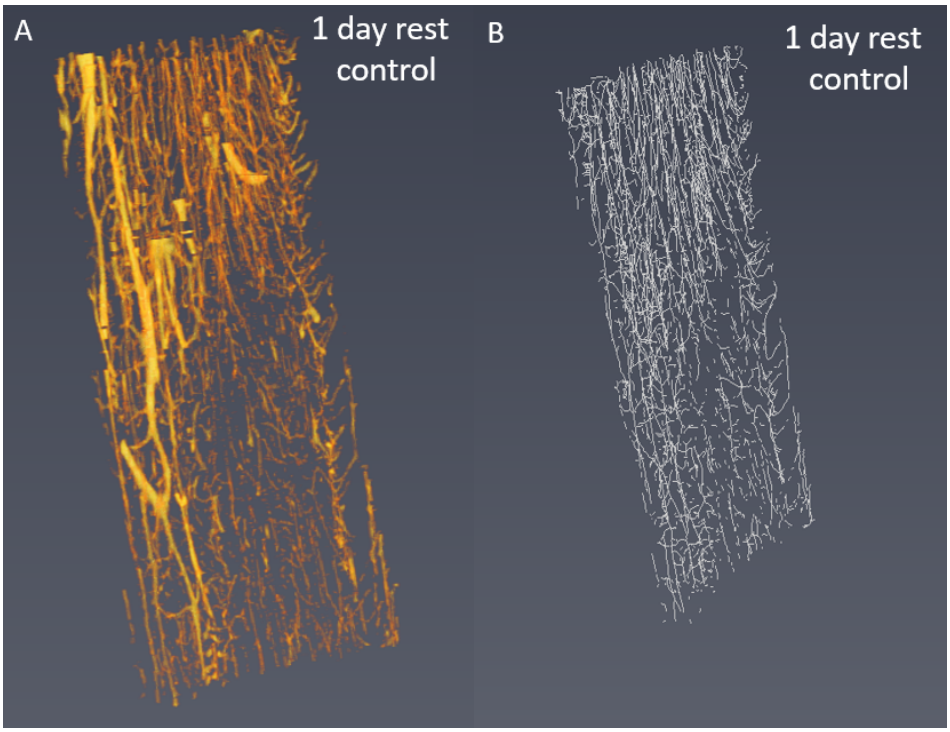

Figure 12: A:3D Volume rendering. B:skeletonization of the specimen in Amira 6.4. The 3D view of the subject was generated based on the image stack of the internal canals, excluding the medullary cavity. Skeletonization can present the segments with lines or tubes, and using node points to indicate branches in the skeleton.

3.5 Data Analyses

Data comparisons between the control and loaded ulnae within the same group were compared using pair-sample t-tests (Origin 2018b, OriginLab Corporation, Northhampton, MA, USA), and data from different groups were compared using two-sample t-test. The significance level used was $\alpha = 0.05$.

3.5.1 Impact load

The peak impact force value of each test was extracted for the statistical analysis using MATLAB. Fracture rates of specimens in each group were also recorded.

3.5.2 Bone morphology

The grayscale images were used to investigate the presence of woven bone formation after fatigue. Using the binarized images of bone, the total bone volume was calculated by adding all binarized voxels and multiplying this value by the volume of each voxel (117.65 μm^3). Moreover, Amira 6.4 was able to generate 3D view of the segmented bone, skeletonize the internal structure. Upon skeletonization.

Upon the generation of the skeleton structure, it can produce analysis of the number of nodes, segments, and the length of each segments can be acquired. Among these measurements, the number of nodes did not reflect the change of the internal structure. The average length of the segments of each specimen did not indicate any structural change neither. However, the number of segments was a reliable indicator of the change that occurred in the specimen. Therefore the number of segments within each skeletonized dataset was analyzed. An increase in segments, relative to the pre-impact condition limbs was used as an indicator of damage because microcracks would appear as additional segments in the skeleton model.

4 Results

4.1 Fatigue

The average number of cycles required to fatigue the ulnae was 1688 ± 1362. There was no correlation between the number of cycles and mass (R = -0.37, Figure 13).

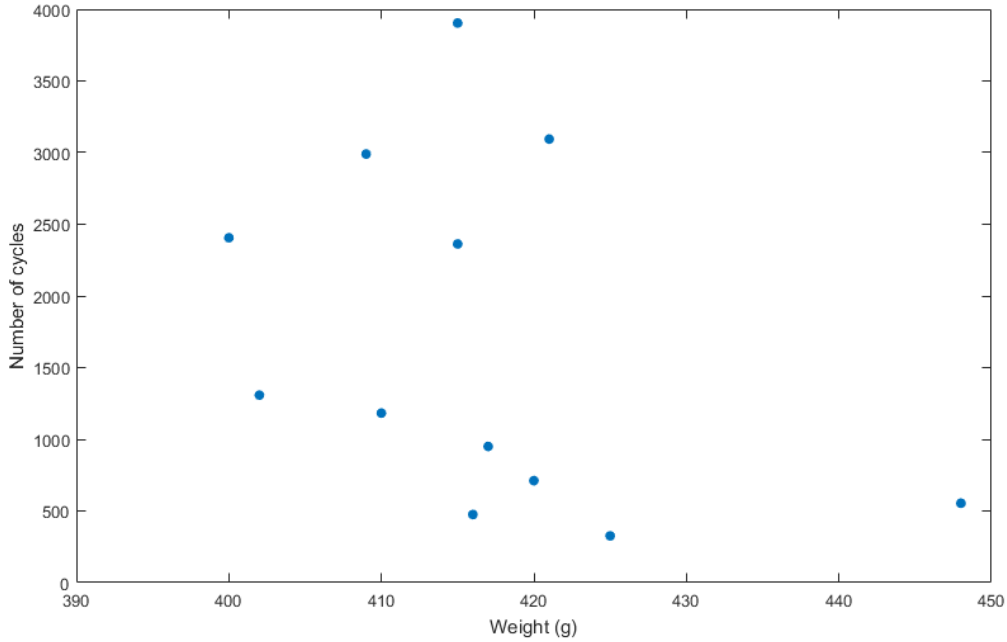

Figure 13: Number of cycles to reach fatigue and the body weight of each subject. There was no strong correlation between them. Larger rats did not always need more cycles to fatigue.

Ulnae exposed to loading and one day of rest were mechanically more compromised than those allowed to rest for more than seven days (Fig. 14). Of the six ulnae within the single rest day group: two were severely damaged before impact testing, three of the remaining four resulted in full catastrophic fracture after impact, and only one remained intact after impact.

In contrast, among the subjects had seven days rest, only one out of six loaded specimens was fractured after the impact. None of the control ulnae was damaged after the impact. Overall, there was only one control ulna resulted in complete fracture in both groups, and the fracture rate of the loaded ulnae was three times greater in the one day rest group (50%) than the other group (16.70%).

The maximum forces of the loaded ulnae ($130.34 \pm 22.37N$) in both group were 25.22% lower than the control ($174.30 \pm 34.65N$) in average. (Figure 15). There was no significant difference in the maximum impact force between the control ($182.67 \pm 36.25N$) and loaded ulnae ($133.95 \pm 19.31N$) after one day

of rest (P = 0.14). However, after seven days rest, the mean impact force was 38.73%higher in the control ulnae compared to the loaded (p = 0.0055).

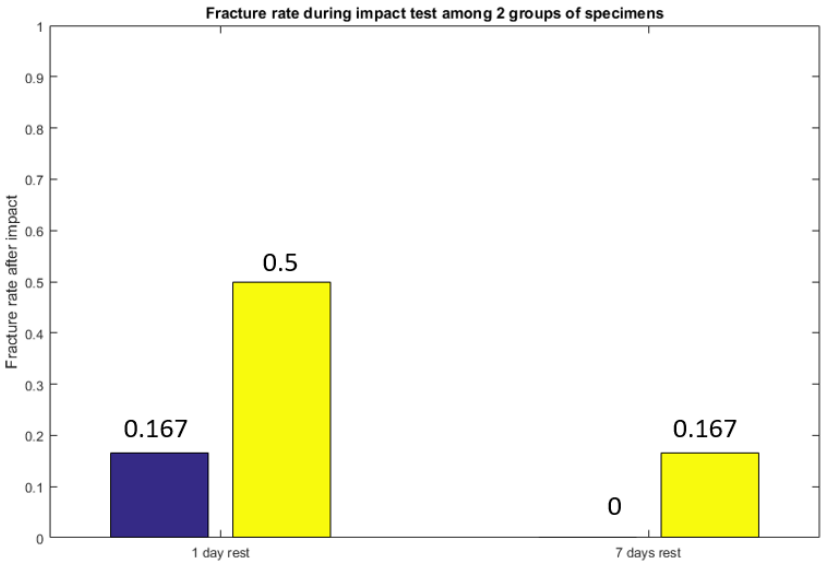

Figure 14: Fracture rate of the specimens during impact loading in two groups. In the group that had one day rest, half of the loaded specimen were fractured during the imapct test, and two were fractured after the cyclic loading. However, the in the group that had seven days rest, only one out of six loaded specimens were fractured during the impact test.

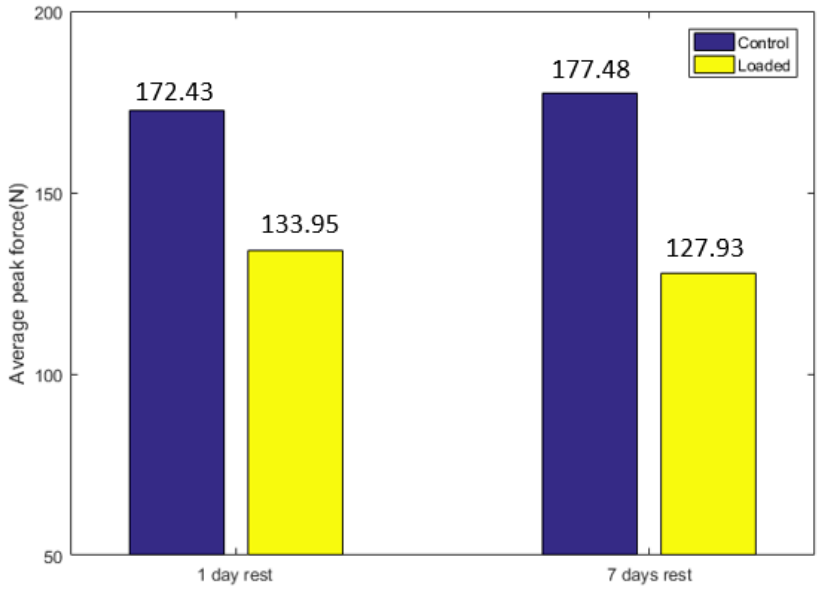

Figure 15: Average peak force of control and loaded specimen in both groups.

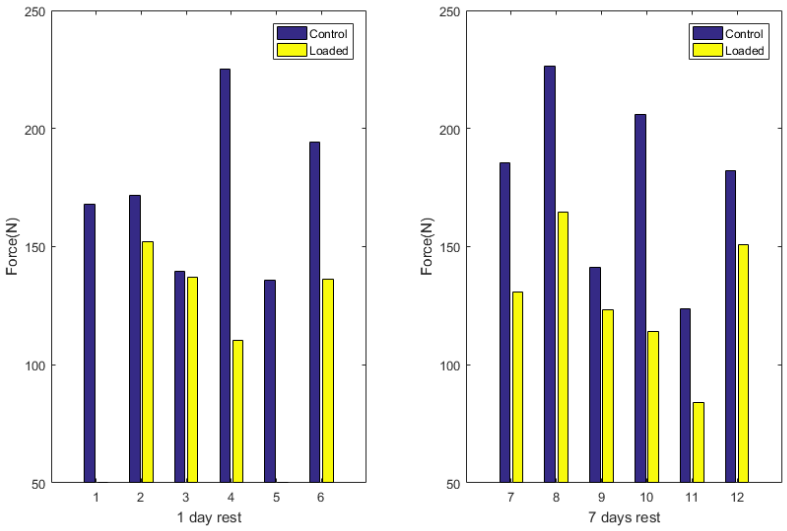

Figure 16: Peak force recorded during impact test of each specimen in both groups. Overall, the control group had higher peak forces than the loaded. Subject 1 and 5 did not have readings for the loaded ulnae due to the fatigue fracture.

4.2 Bone formation with rest

The group with seven days of rest showed noticeable new bone formation in the loaded ulna compared to the control ulna (Figure 17). There was a ring of disorganized bone on the periosteal surface that led to a 4.8% increase in the average cross-sectional area in the loaded samples with seven days rest (1.56 $\pm 0.087 mm^2$) compared to the contralateral control ($1.49 \pm 0.090 mm^2$). However, within the group had one day rest, there was no any noticeable bone formation observed on neither periosteal nor endosteal side.The volume of each scanned specimen also showed a 4.5% increase between the control and loaded ulnae among the subjects had seven days rest. (Figure 18, 19).

The volumes of the control ($7.01 \pm 0.61 mm^3$) and loaded ($6.62 \pm 0.19 mm^3$) specimens in the group after one day of rest were not significantly different ($p = 0.28$). However, the volumes of loaded specimens in the seven days rest group ($7.62 \pm 0.47 mm^3$) were significantly greater than the one day rest group($6.62 \pm 0.19 mm^3$, $P = 0.0021$) by 15.11%.

In general, as the number of segments were nomalized with respect to the volume, the loaded ulnae ($606.84 \pm 325.70/mm^3$) had more segments than the control ($439.78 \pm 164.58/mm^3$) (Figure 20,21). In the group with one day rest, the segments had an average increase of 40.72% and 27.79%in the seven days rest group.

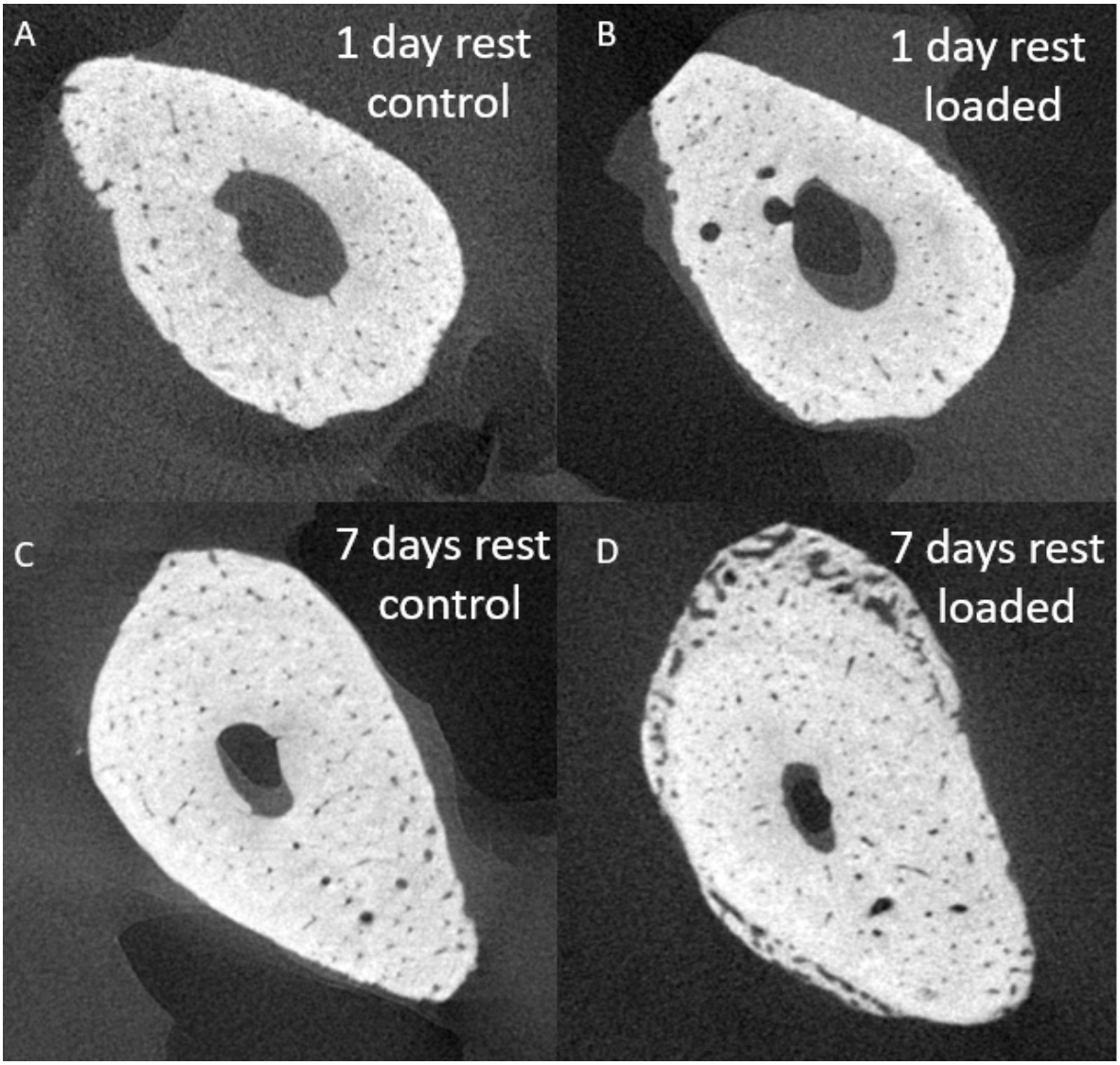

Figure 17: Raw DICOM images of the ulnae. A: control ulna from the subject had one day rest. B: loaded ulna from the subject had one day rest. C: control ulna from the subject had seven days rest. D: loaded ulna from the subject had seven days rest. There was noticeable between the control and loaded ulnae in the group had one day rest. However, with seven days rest, there was formation of woven bone on the periosteal side of the ulna on the loaded ulna but not the control.

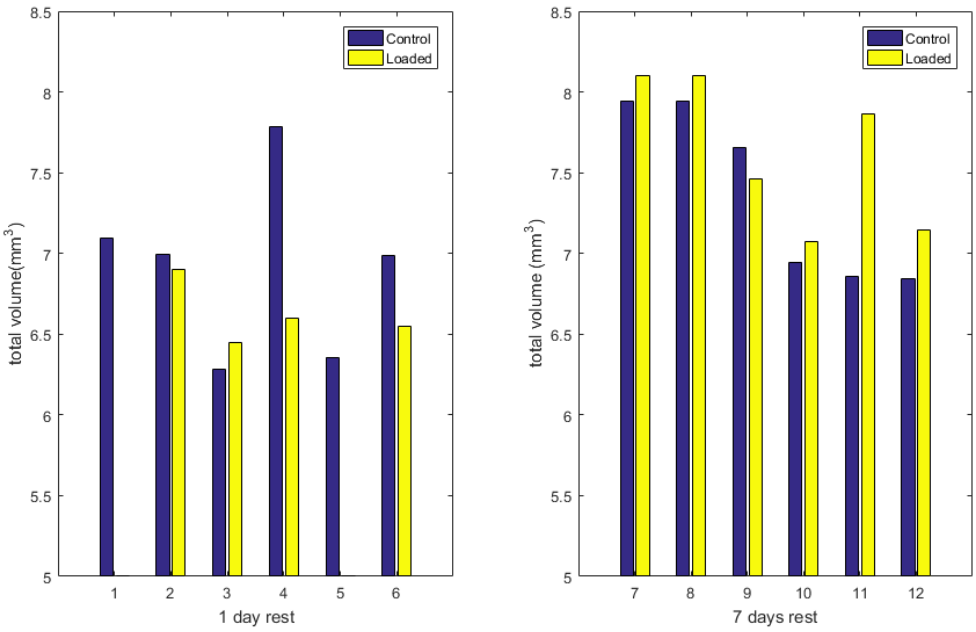

Figure 18: Scanned volume of each specimen among two groups. The volumes of loaded ulnae that had seven days rest were significantly greater than one days. The difference between the control ulnae was not significant. The volume was calculated by multiplying the voxel size with total number of voxels in each image stack.

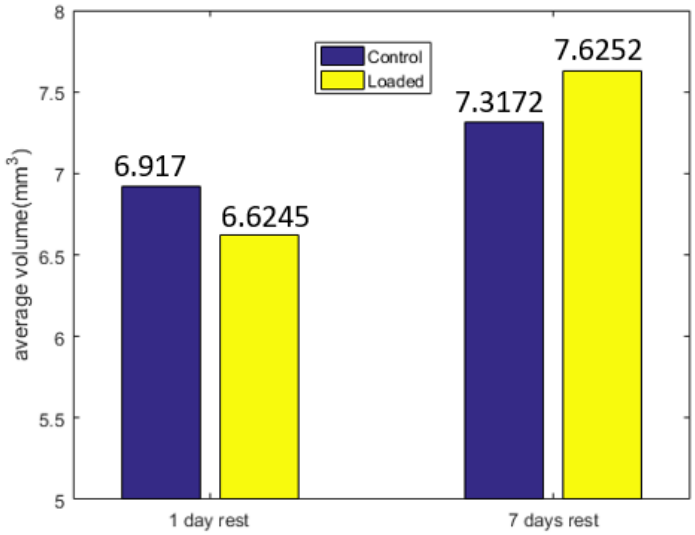

Figure 19: Mean volume of control and loaded ulnae in each group. The mean volume of the loaded ulnae in the group had seven days rest were significantly greater than the other group, but not the control.

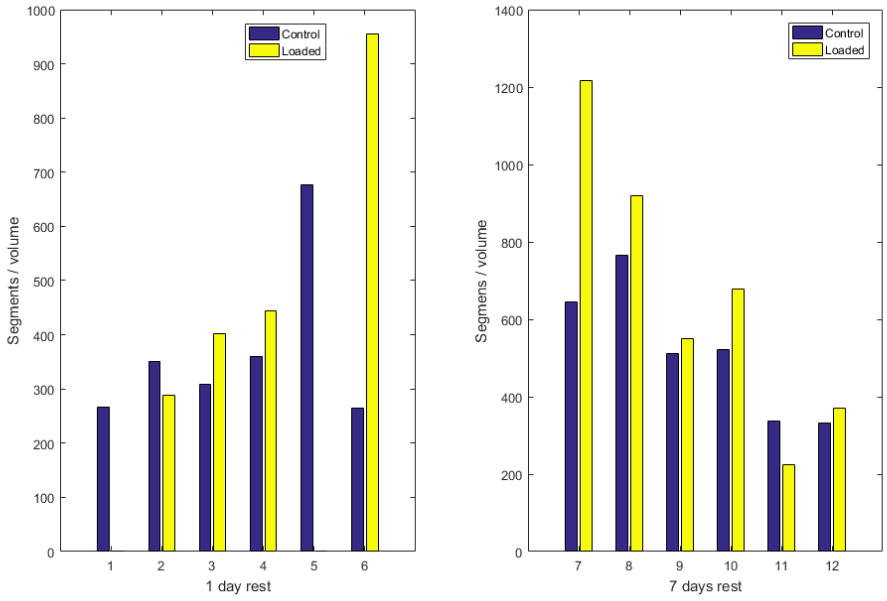

Figure 20: Number of segments of each individual specimen normalized to the volume. The plot shows the number of segments per millimeter cube volume. Subject 1 and 5 did not have loaded specimen due to premature fracture. In most cases, the loaded specimens had greater ratio than the control.

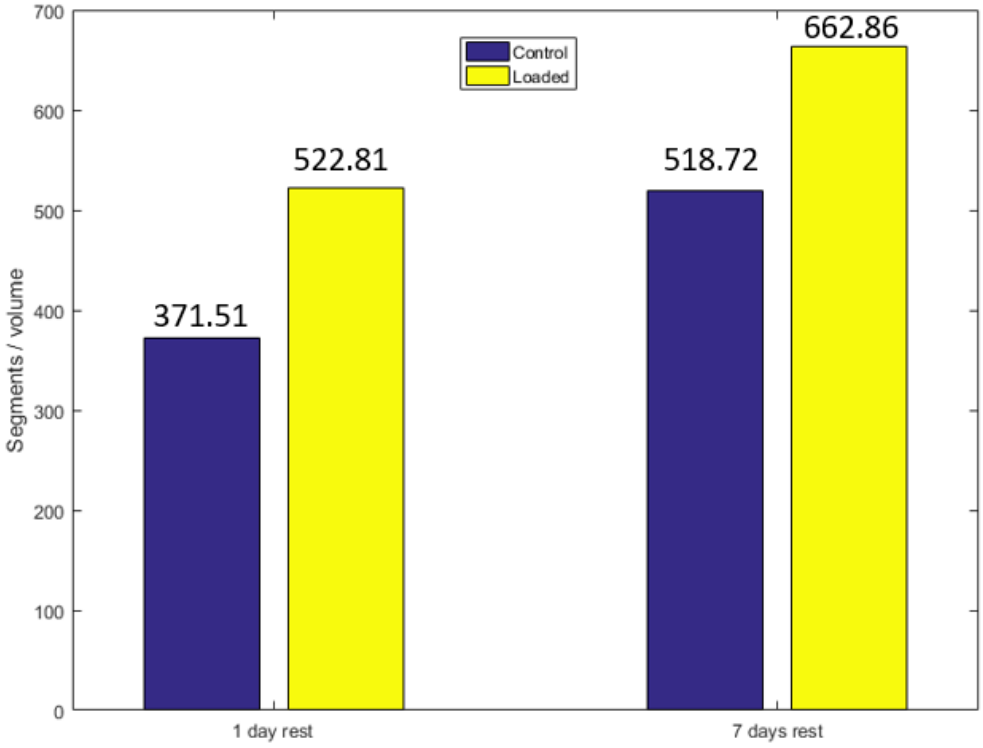

Figure 21: Average number of normalized segments in both control and loaded ulnae in two different groups. The loaded ulnae had a number of segments than the control in both groups.

5 Discussion

According to several previous research, a single bout of cyclic loading with peak force of 0.055N/g body weight on a rat ulna was enough to induce fatigue damage. The slight limping occurred after the loading on some subjects was partially due to the stiffened joint and the anesthesia. There were two abnormal subjects that had rapid increase in the peak displacement during cyclic loading and turned out to be fractured. After the dissection of rats with one day rest, no new bone formation was observed from the microCT scan. However, woven bone formation was identified in the group that had seven days rest from CT scans, which supported our hypothesis that a single bout of loading was enough to induce woven bone formation. The woven bone was identified on the periosteal side but not on the endosteal side. One reason could be that the strain distributed on ulna during the cyclic loading was much greater on the periosteal side than the endosteal. According to previous studies related to cyclic loading of rat ulna [32, 34, 50], this ring of disorganized bone could be woven bone that formed after fatigue loading as a part of the bone remodeling process to repair damage. Uthgenannt [52] stated that, whole bone strength was partially recovered around seven days after the loading, and fully recovered at around fourteen days regardless of initial stress fracture severity. The partial recovery was attributed to the rapid formation of woven bone which was maximal near the ulnar mid-shaft. The results from the impact test also confirmed this point (Figure 14). The subjects that had one day rest showed an 50% fracture rate, however, the subject had seven days rest had only 16.67%. The overall integrity of loaded ulnae in the group with seven days rest was stronger than the one day rest group, whereas there were three loaded specimens fractured among the one day rest group. Although the mean peak force recorded in the loaded specimens with one day rest (133.95N) is slightly greater than the seven days rest (127.93), the fracture rate was certainly enough to prove the partial strength recovery due to the woven bone formation.

DICOM data of the loaded ulnae from seven days rest group clearly indicated woven bone formation on the periosteal of the ulna. It had a unique disorganized pattern and it was much less compact than the cortical bone. Moreover, based on the peak force value of each specimen, it do not seem to provide much support as healthy cortical bone comparing to the control. This decreased resistance to fracture was associated with the accumulation and coalescence of branching arrays of microcracks within the cortxex of the ulna[14]. Although no stain was used nor histomorphometric analysis, the CT scan with resolution of 5μm can provide a detailed view of transverse section at target region, which included the formation of woven bone. However, the scan was not able to cover the whole ulna. More cracks or fracture could potentially occur at other locations along the diaphysis but were not captured.

In this study, we were confident with the techniques that applied to process the image data. The cracks observed in the raw DICOM data were preserved after the binarization (Figure 22). More example im-

ages were attached in the appendices. Many of those cracks were generated from the existing canals or around the medullary cavity, which were common regions of high stress concentration. Previous studies had identified stress fracture across the ulna using histomophormetric analysis, in this study, cracks that generated from the medullary cavity with size from tens to hundreds of microns could be identified.

Skeletonization became a convenient method to visually examine the internal structure of a given biological material. However, the data were sensitive to the noise introduced during the image process. The data showed that loaded ulnae had more normalized segments than the control in general, but the difference was not significant (P = 0.071). We were confident about this result, and the error induced would be approximately 10%, which we would accept for this experiment. The increase in normalized segments confirmed the assumption that fatigue loading would induce microcracks and the coalescence of the microcracks, and also increase the vascularity of the loaded ulnae.

McKenzie and Silva[34] performed microCT scan on irrigated rat forelimbs. The images were taken at 1.6mm of the central ulna starting 1mm distal to the midpoint and 0.4mm proximal to the midpoint. The increase in vascularity can be assessed on day three after a single bout of damaging fatigue loading. The results from the segmentation also confirmed this finding. The mean values of the normalized segment numbers among the seven days rest group in both controlled ($518.72 \pm 170.05/mm^3$) and loaded ($662.86 \pm 359.07/mm^3$) specimens were greater than the one day rest group ($321.37 \pm 43.70/mm^3$, $522.81 \pm 296.09/mm^3$).

There exists noticeable difference between individual rat during the the experiments. Some rats needed much less loading cycles to reach the prescribed peak displacement regardless of body weight. Additionally, even small number of cycles can also induce woven bone formation as long as the peak displacement reached the threshold.

The difference in peak force between controlled and loaded ulnae during impact test within one day rest group was not significantly different. This could be a consequence of the high fracture rate in this group. From the results, it is clear that loaded ulnae had lost some degree of stiffness. It supported the assumption that after experiencing repeated load or exercise, the overall bone mechanical properties will be compromised including stiffness. At this time, enough rest should be given, otherwise the subject would be more prone to bone damage or even fracture.

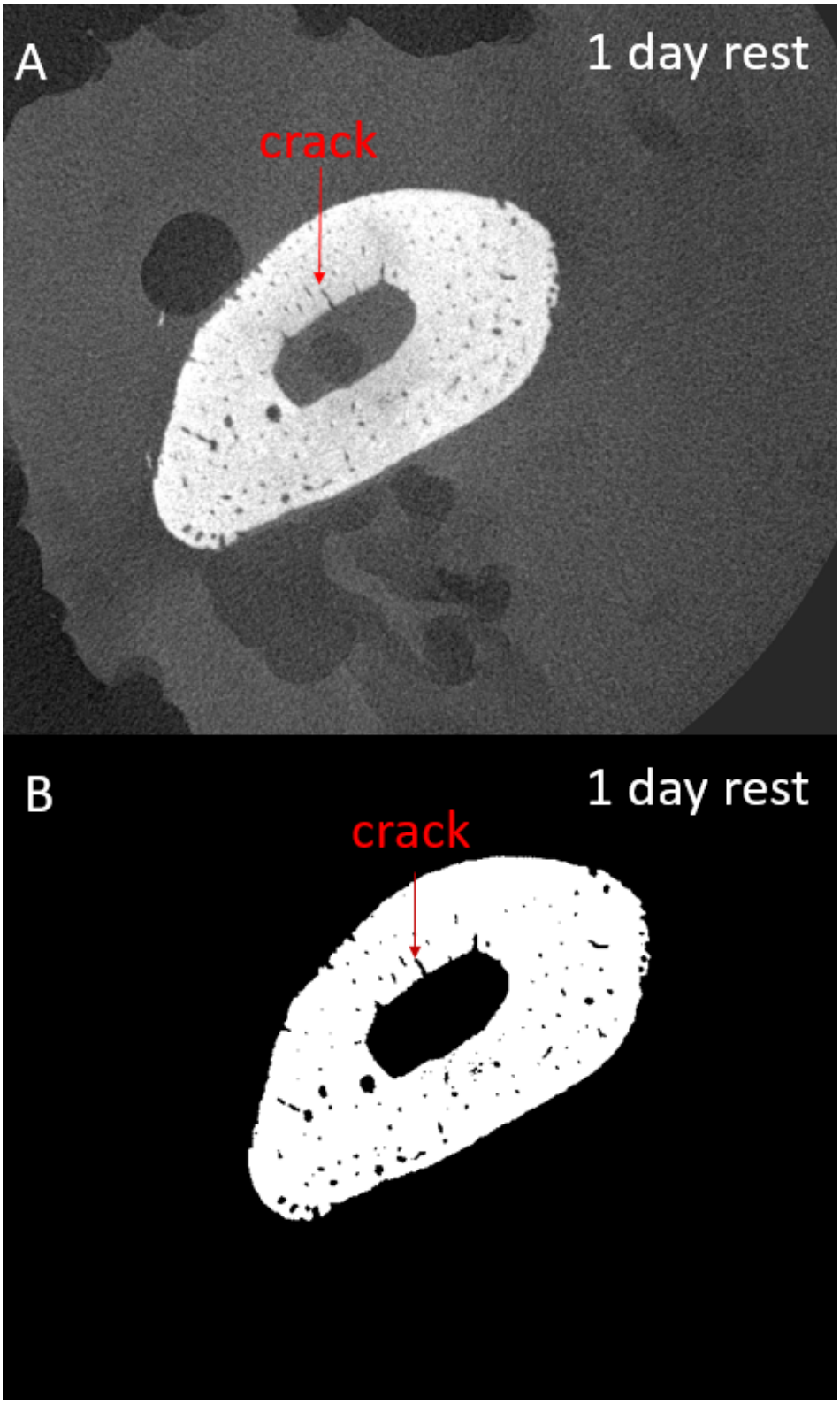

Figure 22: The cracks observed in the raw images from DICOM (top) was preserved after the image process and binarization (bottom), and can be easily identified by eye inspection. The cracks were common among loaded specimens.

6 Limitations

Although there were many studies that focus on the cyclic loading of rat bones in both compression and bending, few were focused on the impact behavior. Many existing researches had investigated the biological influence and anabolic effect of the fatigue loading and how bone cells react to the external stimuli on a cellular level[32, 26, 54, 5]. Additionally, some studies have looked into the change in material and mechanical properties[52, 13, 55]. However, relatively less studies focused the impact loading on biological tissue[18, 44]. One limitation was the difficulty of performing mechanical tests on human bodies in a noninvasive way. Moreover, the age and gender of the donors play an important role in the mechanical properties of the samples. Although the structure of rat bone was similar to human beings', it cannot fully resemble the human bone.

Four rats were ordered prior to the rest subjects to perform a pilot experiment. In vivo CT scan were performed on two of the pilot subjects. However, the in vivo scan did not produce the results we desired. Due to the limitation of the equipment and image resolution, the scan did not present valuable information for this study so the in vivo scan was abandoned for the rest of the study. Additionally, for each bone, the repeated scans would take place at roughly the same region on the bone. Due to the potting quality, first four pilot subjects did not produce acceptable results. Therefore, among the other twelve subjects, all specimen were left dry before and during the potting to secure the solidification process. Afterwards, all specimens were wrapped in gauze that was soaked with PBS solution to rehydrate.

During the impact test, even though lubrication oil was used to decrease the friction, there could still be resistance. The maximum velocity of the weight was limited to 1.98m/s, since the weight was accelerated by gravity only. Additionally, the sampling frequency of the load cell had a limit of 40 kHz which may not be able to record the maximum force in all trials and thus potentially resulted in errors among some of the data. Furthermore, because of the difficulty of machining customized weights, the potential energy of the load might deviate from the expected value by a small amount. Rat was a good model for many experiments, but their bone size was limited. As a result, the specimens can be easily damaged during dissection comparing to other larger subjects such as bovine bones. Additionally, smaller bone size was more sensitive to human error, for example the potting position of each specimen might be slightly different, which was difficult to notice by eye inspection. On the other hand, due to the variance between rats, some subjects reached the prescribed peak displacement much faster than others, and resulted in much weakened or even fractured ulnae.

All specimens were scanned on the Deben with the customized bottom fixture. However, due to human error, the specimens were not able to be scanned in the exact same positions. As a result, the scans before and after the impact test do not capture the exact same region. There was slight translation

and rotation occurred between the scans, even though all specimens were placed at the same coordinate positions during two rounds of scanning to minimize the error. Additionally, the size of view is limited for the resolution. As a consequence, the common region shared across all scans was difficult to identify precisely due to the variation in size and geometry of each specimen. The region of view generally covers a 5mm window from distal end to one third up the diaphysis. We were not able to scan the full size of the ulna given the restraints on time and condition of the equipment.

Due to the the limitations stated above, we did not have an efficient way to identify a crack or crack formation except visual inspection. In most cases, the difference between a in-plane canal and crack is not so obvious. Additionally, as the CT images were processed, an inevitable amount of noise is introduced. But we were confident about the images obtained. We were able to identify the cracks that were in the scale of tens to hundreds of microns.

7 Conclusion

Fatigue properties and impact response are both important mechanical aspects of biological tissues. In fact, the the structural failure of the biological system and most mechanical systems occur rapidly and were frequently due to impacts of varying velocity in stead of static loading[33]. Indeed, impact load plays an important role in dynamic failure. The in vivo bone properties in long bones can be examined through the stress wave propagation generated by impact force[57].

The objective of this study was to combine cyclic and impact loading together and examine the effect of cyclic fatigue loading on the impact response of the specimens. This study can potentially provide more insights on how the bone response to external impact when it was fatigued or overused. Therefore, athletes and their coaches can arrange the training routines more efficiently based on the recovery condition.

The hypothesis was confirmed that a single bout of cyclic loading was enough to cause the microdamage and the woven bone formation. Additionally, it was proved that the woven bone can resist impact load better than the specimens without woven bone based on the fracture rate. This study can serve as a baseline for future study of complex loading condition on other biological materials or bones from larger animals.

For the future study, larger animal subjects can be tested for analysis in a greater scale. More complicated stress and strain analysis can also be performed. Additionally, the potting material and fixtures can be modified to provide a more robust and uniform testing environment. Furthermore, the impact test can be improved to have multiple impact velocity instead of one. This study chose to focus on the mechanical side of the bone, and did not investigate the change in cellular level. With the advancement in technology, more sophisticated equipment and image process techniques will be developed and used to process the microCT data and produce more accurate results. On the other hand, the change occurs on the cellular level is also worth further analysis.

8 References

[1] Cedo M Bagi, Nels Hanson, Catharine Andresen, Richard Pero, Roland Lariviere, Charles H Turner, and Andres Laib. The use of micro-ct to evaluate cortical bone geometry and strength in nude rats: correlation with mechanical testing, pqct and dxa. *Bone*, 38(1):136–144, 2006.

[2] Thomas J Beck, Christopher B Ruff, Firas A Mourtada, Richard A Shaffer, Karen Maxwell-Williams, George L Kao, David J Sartoris, and Stephanie Brodine. Dual-energy x-ray absorptiometry derived structural geometry for stress fracture prediction in male us marine corps recruits. *Journal of Bone and Mineral Research*, 11(5):645–653, 1996.

[3] TJ Beck, CB Ruff, Richard A Shaffer, K Betsinger, DW Trone, and SK Brodine. Stress fracture in military recruits: gender differences in muscle and bone susceptibility factors. *Bone*, 27(3):437–444, 2000.

[4] Kim L Bennell, Susan A Malcolm, Shane A Thomas, Sally J Reid, Peter D Brukner, Peter R Ebeling, and John D Wark. Risk factors for stress fractures in track and field athletes: a twelve-month prospective study. *The American journal of sports medicine*, 24(6):810–818, 1996.

[5] V Bentolila, TM Boyce, DP Fyhrie, R Drumb, TM Skerry, and Mitchell B Schaffler. Intracortical remodeling in adult rat long bones after fatigue loading. *Bone*, 23(3):275–281, 1998.

[6] David B Burr, Mark R Forwood, David P Fyhrie, R Bruce Martin, Mitchell B Schaffler, and Charles H Turner. Bone microdamage and skeletal fragility in osteoporotic and stress fractures. *Journal of Bone and Mineral Research*, 12(1):6–15, 1997.

[7] David B Burr, C Milgrom, D Fyhrie, M Forwood, M Nyska, A Finestone, S Hoshaw, E Saiag, and A Simkin. In vivo measurement of human tibial strains during vigorous activity. *Bone*, 18(5):405–410, 1996.

[8] Dennis R Carter, William E Caler, Dan M Spengler, and Victor H Frankel. Fatigue behavior of adult cortical bone: the influence of mean strain and strain range. *Acta Orthopaedica Scandinavica*, 52(5):481–490, 1981.

[9] DR Carter and Wilson C Hayes. Fatigue life of compact bone—i effects of stress amplitude, temperature and density. *Journal of Biomechanics*, 9(1):IN7, 1976.

[10] DR Carter and Wilson C Hayes. Compact bone fatigue damage—i. residual strength and stiffness. *Journal of Biomechanics*, 10(5-6):325–337, 1977.

[11] A Chamay and P Tschantz. Mechanical influences in bone remodeling. experimental research on wolff's law. *Journal of biomechanics*, 5(2):173–180, 1972.

[12] Krishan Kumar Chawla and MA Meyers. *Mechanical behavior of materials*. Prentice Hall, 1999.

[13] SA Colopy, J Benz-Dean, JG Barrett, SJ Sample, Y Lu, NA Danova, VL Kalscheur, R Vanderby, MD Markel, and P Muir. Response of the osteocyte syncytium adjacent to and distant from linear microcracks during adaptation to cyclic fatigue loading. *Bone*, 35(4):881–891, 2004.

[14] NA Danova, SA Colopy, CL Radtke, VL Kalscheur, MD Markel, R Vanderby, RP McCabe, AJ Escarcega, and P Muir. Degradation of bone structural properties by accumulation and coalescence of microcracks. *Bone*, 33(2):197–205, 2003.

[15] William S Enns-Bray, Stephen J Ferguson, and Benedikt Helgason. Strain rate dependency of bovine trabecular bone under impact loading at sideways fall velocity. *Journal of Biomechanics*, 2018.

[16] F Gaynor Evans and Milton Lebow. Strength of human compact bone under repetitive loading. *Journal of applied physiology*, 10(1):127–130, 1957.

[17] Celal Evci and Müfit Gülgeç. An experimental investigation on the impact response of composite materials. *International Journal of Impact Engineering*, 43:40–51, 2012.

[18] PC Fehling, L Alekel, J Clasey, A Rector, and RJ Stillman. A comparison of bone mineral densities among female athletes in impact loading and active loading sports. *Bone*, 17(3):205–210, 1995.

[19] MARK R Forwood, ICHIRO Owan, YUICHI Takano, and CHARLES H Turner. Increased bone formation in rat tibiae after a single short period of dynamic loading in vivo. *American Journal of Physiology-Endocrinology and Metabolism*, 270(3):E419–E423, 1996.

[20] JD Frank, M Ryan, VL Kalscheur, CP Ruaux-Mason, RR Hozak, and P Muir. Aging and accumulation of microdamage in canine bone. *Bone*, 30(1):201–206, 2002.

[21] MAR Freeman, RC Todd, and CJ Pirie. The role of fatigue in the pathogenesis of senile femoral neck fractures. *Bone & Joint Journal*, 56(4):698–702, 1974.

[22] Harold M Frost. Bone "mass" and the "mechanostat": a proposal. *The anatomical record*, 219(1):1–9, 1987.

[23] John W Heath. *Wheater's functional histology: a text and colour atlas*. Churchill Livingstone, 1993.

[24] J Hert, M Liskova, and J Landa. Reaction of bone to mechanical stimuli. 1. continuous and intermittent loading of tibia in rabbit. *Folia morphologica*, 19(3):290–300, 1971.

[25] Yeou-Fang Hsieh and Matthew J Silva. In vivo fatigue loading of the rat ulna induces both bone formation and resorption and leads to time-related changes in bone mechanical properties and density. *Journal of Orthopaedic Research*, 20(4):764–771, 2002.

[26] Yeou-Fang Hsieh and Charles H Turner. Effects of loading frequency on mechanically induced bone formation. *Journal of Bone and Mineral Research*, 16(5):918–924, 2001.

[27] Laith M Jazrawi, Robert J Majeska, Michael L Klein, Eric Kagel, Lennart Stromberg, and Thomas A Einhorn. Bone and cartilage formation in an experimental model of distraction osteogenesis. *Journal of orthopaedic trauma*, 12(2):111–116, 1998.

[28] Lent C Johnson. Histogenesis of stress fracture. *J. Bone Joint Surg., A*, 45:1542, 1963.

[29] Lance E Lanyon and CT Rubin. Static vs dynamic loads as an influence on bone remodelling. *Journal of biomechanics*, 17(12):897–905, 1984.

[30] LE Lanyon, WGJ Hampson, AE Goodship, and JS Shah. Bone deformation recorded in vivo from strain gauges attached to the human tibial shaft. *Acta Orthopaedica Scandinavica*, 46(2):256–268, 1975.

[31] JM Lappe, MR Stegman, and RR Recker. The impact of lifestyle factors on stress fractures in female army recruits. *Osteoporosis international*, 12(1):35–42, 2001.

[32] Sarah H McBride and Matthew J Silva. Adaptive and injury response of bone to mechanical loading. *BoneKEy Reports*, 1, 2012.

[33] James H McElhaney. Dynamic response of bone and muscle tissue. *Journal of applied physiology*, 21(4):1231–1236, 1966.

[34] Jennifer A McKenzie and Matthew J Silva. Comparing histological, vascular and molecular responses associated with woven and lamellar bone formation induced by mechanical loading in the rat ulna. *Bone*, 48(2):250–258, 2011.

[35] Elise F Morgan, Harun H Bayraktar, and Tony M Keaveny. Trabecular bone modulus–density relationships depend on anatomic site. *Journal of biomechanics*, 36(7):897–904, 2003.

[36] S Mori and DB Burr. Increased intracortical remodeling following fatigue damage. *Bone*, 14(2):103–109, 1993.

[37] Satoshi Mori, Jiliang Li, and Yoji Kawaguchi. The histological appearance of stress fractures. In *Musculoskeletal fatigue and stress fractures*, pages 151–159. CRC Press, Boca Raton, 2001.

[38] CD Nash. Fatigue of self-healing structures. *A generalized theory of fatigue*, 1966.

[39] AN Natali and EA Meroi. A review of the biomechanical properties of bone as a material. *Journal of biomedical engineering*, 11(4):266–276, 1989.

[40] Frank Henry Netter, Edmund S Crelin, Frederick S Kaplan, and Russell Thomas Woodburne. *Musculoskeletal system: a compilation of paintings. Anatomy, physiology, and metabolic disorders*, volume 1. Ciba-Geigy Corporation, 1987.

[41] Matthew J Olszta, Xingguo Cheng, Sang Soo Jee, Rajendra Kumar, Yi-Yeoun Kim, Michael J Kaufman, Elliot P Douglas, and Laurie B Gower. Bone structure and formation: a new perspective. *Materials Science and Engineering: R: Reports*, 58(3):77–116, 2007.

[42] Jerry L Prather, MARTIN L Nusynowitz, HARRY A Snowdy, ALAN D Hughes, WILLIAM H McCartney, and RAYMOND J Bagg. Scintigraphic findings in stress fractures. *The Journal of bone and joint surgery. American volume*, 59(7):869–874, 1977.

[43] EL Radin. Trabecular microfractures in response to stress: the possible mechanism of wolff's law. In *Proceedings of the 12th Congress of the International Society of Orthopaedic Surgery and Traumatology, Tel Aviv*, volume 59, 1972.

[44] Eric L Radin, Howard G Parker, James W Pugh, Robert S Steinberg, Igor L Paul, and Robert M Rose. Response of joints to impact loading—iii: Relationship between trabecular microfractures and cartilage degeneration. *Journal of biomechanics*, 6(1):51–54, 1973.

[45] Clinton T Rubin and LE Lanyon. Regulation of bone formation by applied dynamic loads. *JBJS*, 66(3):397–402, 1984.

[46] MB Schaffler, K Choi, and C Milgrom. Aging and matrix microdamage accumulation in human compact bone. *Bone*, 17(6):521–525, 1995.

[47] Tien-Wei Shyr and Yu-Hao Pan. Impact resistance and damage characteristics of composite laminates. *Composite structures*, 62(2):193–203, 2003.

[48] AE Tami, P Nasser, MB Schaffler, and ML Tate. Noninvasive fatigue fracture model of the rat ulna. *Journal of Orthopaedic Research*, 21(6):1018–1024, 2003.

[49] CH Turner, MP Akhter, DM Raab, DB Kimmel, and RR Recker. A noninvasive, in vivo model for studying strain adaptive bone modeling. *Bone*, 12(2):73–79, 1991.

[50] Charles H Turner, MR Forwood, J-Y Rho, and T Yoshikawa. Mechanical loading thresholds for lamellar and woven bone formation. *Journal of bone and mineral research*, 9(1):87–97, 1994.

[51] Charles H Turner and Alexander G Robling. Exercise as an anabolic stimulus for bone. *Current pharmaceutical design*, 10(21):2629–2641, 2004.

[52] Brian A Uthgenannt, Michael H Kramer, Joyce A Hwu, Brigitte Wopenka, and Matthew J Silva. Skeletal self-repair: stress fracture healing by rapid formation and densification of woven bone. *Journal of Bone and Mineral Research*, 22(10):1548–1556, 2007.

[53] Brian A Uthgenannt and Matthew J Silva. Use of the rat forelimb compression model to create discrete levels of bone damage in vivo. *Journal of biomechanics*, 40(2):317–324, 2007.

[54] Olivier Verborgt, Gary J Gibson, and Mitchell B Schaffler. Loss of osteocyte integrity in association with microdamage and bone remodeling after fatigue in vivo. *Journal of bone and mineral research*, 15(1):60–67, 2000.

[55] Stuart J Warden, Julie A Hurst, Megan S Sanders, Charles H Turner, David B Burr, and Jiliang Li. Bone adaptation to a mechanical loading program significantly increases skeletal fatigue resistance. *Journal of bone and mineral research*, 20(5):809–816, 2005.

[56] I Wolff, JJ Van Croonenborg, HCG Kemper, PJ Kostense, and JWR Twisk. The effect of exercise training programs on bone mass: a meta-analysis of published controlled trials in pre-and postmenopausal women. *Osteoporosis international*, 9(1):1–12, 1999.

[57] Fook Yen Wong, Subrata Pal, and Subrata Saha. The assessment of in vivo bone condition in humans by impact response measurement. *Journal of biomechanics*, 16(10):849–856, 1983.

Appendix A Supplemental Image Process Results

More images from the experiments can confirm the quality of the image process steps (Figure 23, 24, 25).

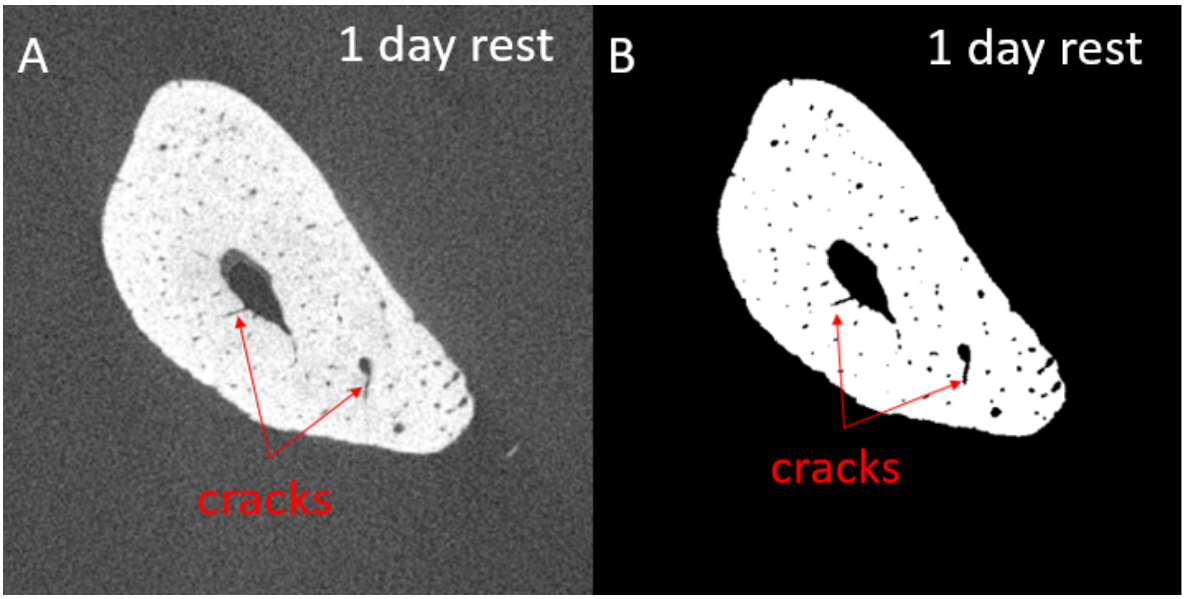

Figure 23: A:cracks from a loaded ulna in the group had 24 hours rest identified in raw DICOM image. B: same cracks were preserved after image process.

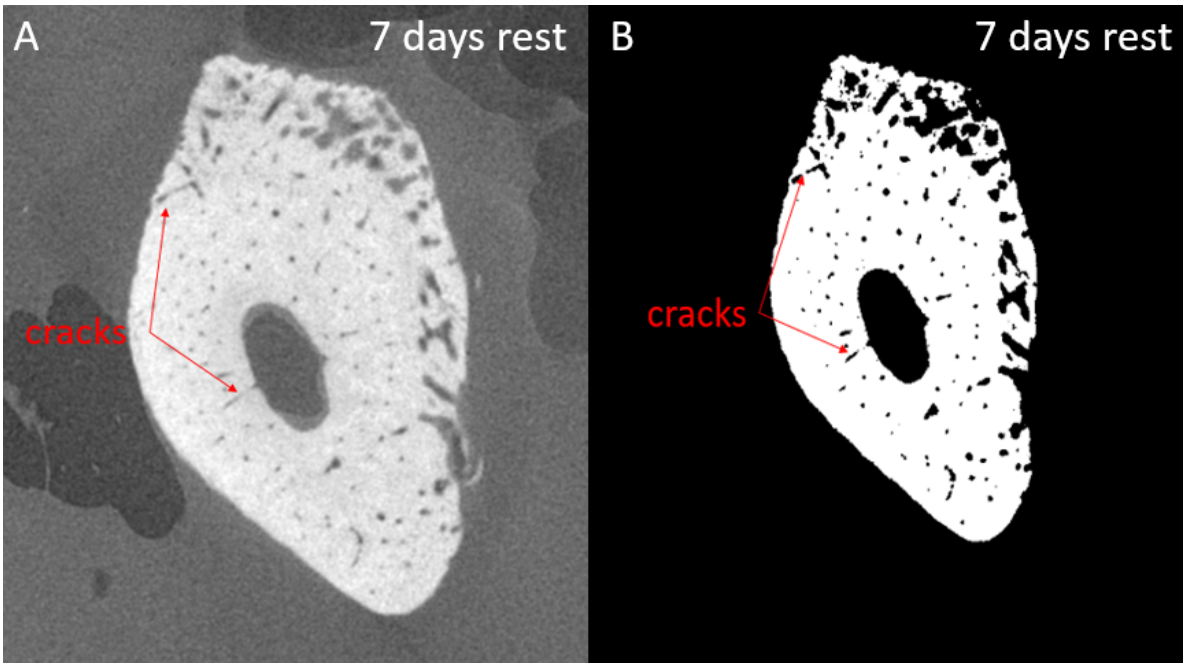

Figure 24: A:cracks from a loaded ulna in the group had 24 hours rest identified in raw DICOM image. B: same cracks were preserved after image process. The woven bone was also preserved after the image process.

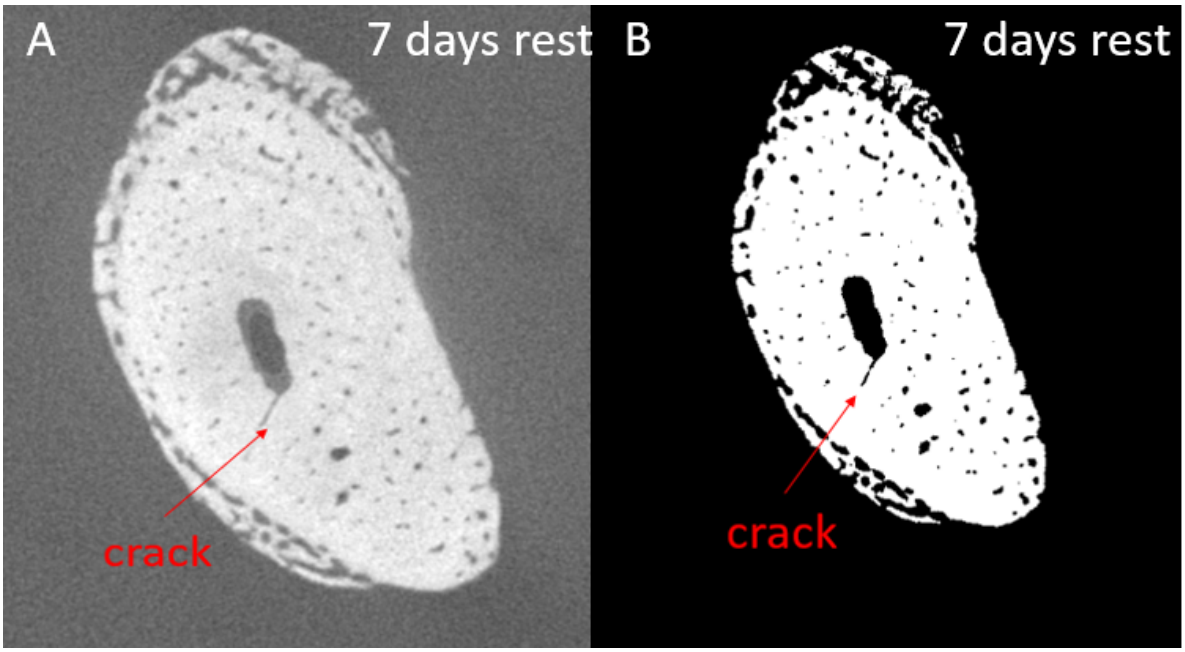

Figure 25: A:cracks from a loaded ulna in the group had 24 hours rest identified in raw DICOM image. B: same cracks were preserved after image process. The woven bone was also preserved after the image process.

Amira 6.4 generates both the 3D volume view and the skeletonization from the image stack. Visualization of the internal structure is important to understand the mechanical properties of the bone (Figure 26). The skeletonization results ware subjected to some level of inevitable noise approximately 10%.

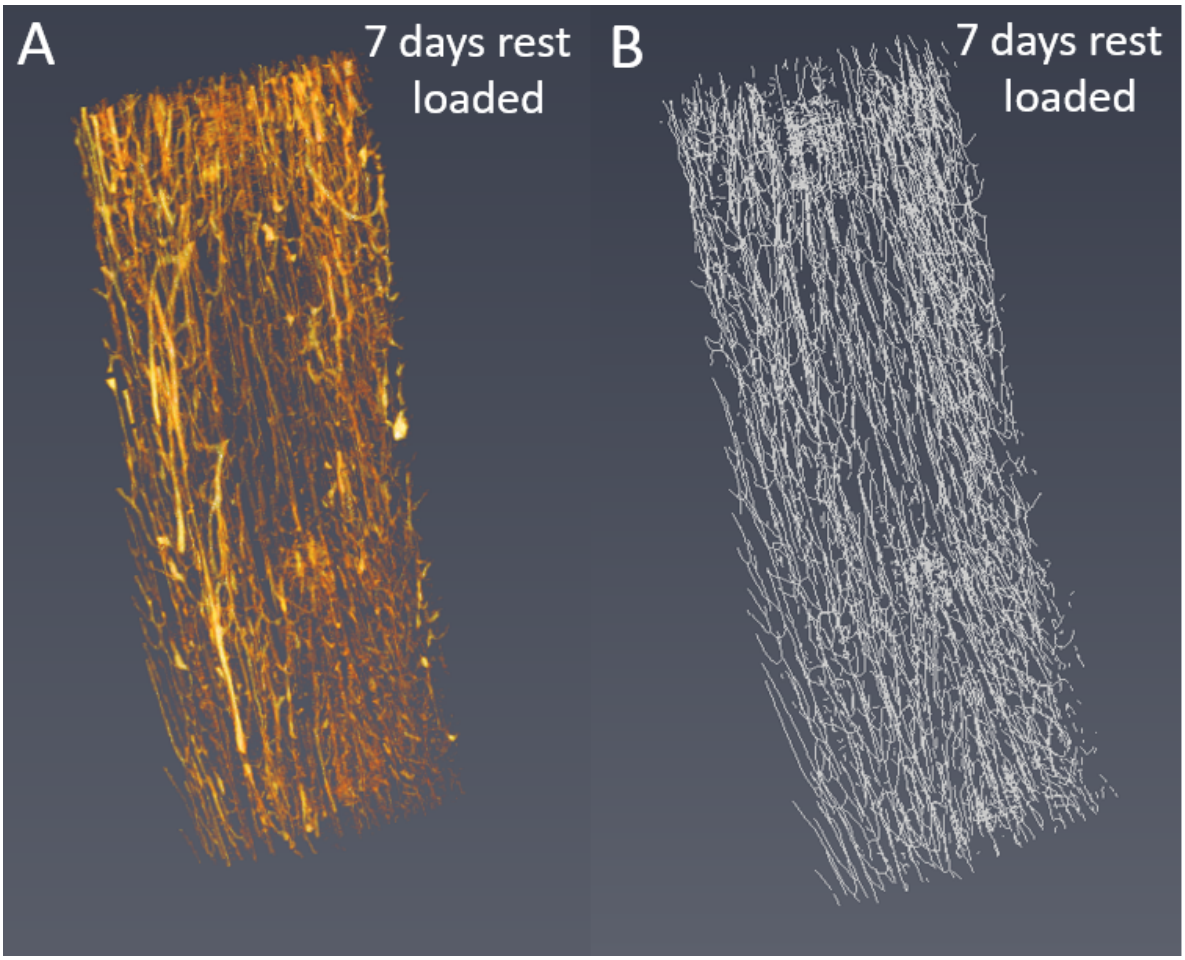

Figure 26: Another example of 3D volume rendering and skeletonization of the specimen in Amira 6.4. A: the 3D view of the subject was generated based on the image stack of the internal canals, excluding the medullary cavity. B: skeletonization of the internal structure, represented by line segments.